PNAS RESEARCH ARTICLE | MICROBIOLOGY OPEN ACCESS

Immunoglobulin G subclasses confer protection against *Staphylococcus aureus* bloodstream dissemination through distinct mechanisms in mouse models

Xinhai Chen[a,b], Haley Gula[a,1], Tonu Pius[a,1], Chong Ou[c], Margaryta Gomozkova[c], Lai-Xi Wang[c], Olaf Schneewind[a,2], and Dominique Missiakas[a,3]

Edited by Dennis Kasper, Harvard Medical School, Boston, MA; received December 8, 2022; accepted March 3, 2023

Antibodies bind target molecules with exquisite specificity. The removal of these targets is mediated by the effector functions of antibodies. We reported earlier that the monoclonal antibody (mAb) 3F6 promotes opsonophagocytic killing of *Staphylococcus aureus* in blood and reduces bacterial replication in animals. Here, we generated mouse immunoglobulin G (mIgG) subclass variants and observed a hierarchy in protective efficacy 3F6-mIgG2a > 3F6-mIgG1 ≥ 3F6-mIgG2b >> 3F6-mIgG3 following bloodstream challenge of C57BL/6J mice. This hierarchy was not observed in BALB/cJ mice: All IgG subclasses conferred similar protection. IgG subclasses differ in their ability to activate complement and interact with Fcγ receptors (FcγR) on immune cells. 3F6-mIgG2a-dependent protection was lost in FcγR-deficient, but not in complement-deficient C57BL/6J animals. Measurements of the relative ratio of FcγRIV over complement receptor 3 (CR3) on neutrophils suggest the preferential expression of FcγRIV in C57BL/6 mice and of CR3 in BALB/cJ mice. To determine the physiological significance of these differing ratios, blocking antibodies against FcγRIV or CR3 were administered to animals before challenge. Correlating with the relative abundance of each receptor, 3F6-mIgG2a-dependent protection in C57BL/6J mice showed a greater reliance for FcγRIV while protection in BALB/cJ mice was only impaired upon neutralization of CR3. Thus, 3F6-based clearance of *S. aureus* in mice relies on a strain-specific contribution of variable FcγR- and complement-dependent pathways. We surmise that these variabilities are the result of genetic polymorphism(s) that may be encountered in other mammals including humans and may have clinical implications in predicting the efficacy of mAb-based therapies.

antibody | effector function | opsonophagocytosis | *Staphylococcus aureus* | neutrophil

Significance

Antigen–immunoglobulin complexes are recognized by Fcγ receptors (FcγRs) coexpressed as activating and inhibitory (A/I) receptors on the same cells, in ratios that govern the outcome of immune responses. Antigen–immunoglobulin complexes can also activate complement for recognition by complement receptors (CRs). Here, we find that protection with the same therapeutic antibody targeting *Staphylococcus aureus* is achieved in an FcγR-dependent manner in C57BL/6J mice and CR3-dependent manner in BALB/cJ mice. Protection was associated with the preferential expression of FcγRIV on C57BL/6J neutrophils and CR3 on BALB/cJ neutrophils. Thus, both the A/I FcγRs ratio and the relative abundance of FcγRs over CRs impact the effector activity of an antibody and the mechanism of elimination of immune complexes.

Staphylococcus aureus is a gram-positive bacterium that colonizes the skin and nares of humans and is the most frequent cause of skin and soft tissue infections (1–3). *S. aureus* colonization raises the risk of infections, as demonstrated by the fact that 80% of bloodstream infection isolates are genetically indistinguishable from *S. aureus* cultured from nasal swabs upon admission to the hospital (4). The ability of *S. aureus* to survive in the bloodstream promotes rapid dissemination to many different sites, causing severe disease manifestations such as sepsis, infective endocarditis, and deep-seated abscesses in virtually every organ tissue (1–3, 5). The use of antibiotics to promote decolonization and prophylaxis of nosocomial disease is associated with the emergence and spread of drug-resistant strains designated MRSA (methicillin-resistant *S. aureus*) that cause difficult-to-treat infections with increased therapeutic failure and mortality rates (6, 7). To overcome this public health problem, significant effort has been directed toward developing alternatives to antibiotics including therapeutic antibodies (8).

Active immunization, the elicitation of protective antibodies, and passive immunization, the transfer of antibodies, have dramatically improved the outcome of infectious diseases. Successful immunization requires the identification of key protective antigens (9). Narrowing down the "protective antigens" of the human pathogen *S. aureus* has proven more challenging as evidenced by several failed clinical trials toward the development of vaccines and antibody therapeutics (10, 11). It has been suggested that the constant exposure to *S. aureus* through colonization or past infections, may account for the ineffectiveness of active and passive immunizations (12–15). One assumption is that the pathogen elicits nonprotective antibodies that compete with protective antibodies of active or passive immunizations (16). Another possibility is that key antigens may be able to simply escape host recognition. We proposed earlier that Staphylococcal protein A (SpA) is one such antigen (17). SpA is a conserved and abundant protein

Competing interest statement: The authors have organizational affiliations to disclose, D.M. is a founder of ImmunArtes LLC., a University of Chicago start-up company that seeks to develop immune therapeutics against *S. aureus*. X.C., D.M., and O.S. are co-inventors of patents that describe monoclonal antibodies as therapeutics against *S. aureus*.

This article is a PNAS Direct Submission.

[1]H.G. and T.P. contributed equally to this work.

[2]Deceased May 26, 2019.

[3]To whom correspondence may be addressed. Email: dmissiak@bsd.uchicago.edu.

This article contains supporting information online at https://www.pnas.org/lookup/suppl/doi:10.1073/pnas.2220765120/-/DCSupplemental.

Published March 27, 2023.

displayed on the cell surface where it binds the Fcγ domain of IgG via several Immunoglobulin-binding domains (IgBDs) to block complement component C1q recruitment and complement-dependent opsonophagocytic uptake of bacteria (18–21). SpA-IgBDs also bind the variant heavy chain 3 (V_H3) of soluble antibodies and V_H3-IgM B cell receptor to prevent the development of neutralizing anti-*S. aureus* responses (17, 22–26). Carefully applied molecular engineering yielded non-functional SpA variants that elicit SpA-neutralizing antibodies (27, 28). This technology was exploited to derive the monoclonal antibody (mAb) 3F6 that blocks SpA binding to its ligands Fcγ and V_H3-Fab (20, 29). Using a recombinant human IgG1 variant, we demonstrated earlier that N297-linked glycosylation of Fcγ is required for 3F6 protection against *S. aureus* bloodstream infection in mice (30). Protection was further improved by engineering 3F6-hIgG1 to prevent SpA from blocking Fcγ and C1q interactions (31).

Exploiting antibodies for the treatment of infections requires the identification of protective antigens as well as an understanding of the mechanisms involved in effector functions carried out by the constant region (Fcγ) of immunoglobulins. In mice, all IgG subclasses may engage with C1q and four Fcγ receptors (FcγRs) known as FcγRI, FcγRIIb, FcγRIII, and FcγRIV, with variable affinities ranging from negligible to high (32, 33). To investigate the impact of antibody's constant region in preventing *S. aureus* bloodstream dissemination, we generated recombinant mouse IgG1 (mIgG1), IgG2a (mIgG2a), IgG2b (mIgG2b), and IgG3 (mIgG3) variants of 3F6 and performed passive immunization studies in two mouse lines. We found that protection varied with the mouse strain and 3F6 subclass. We observed strain-specific differences in relative levels of surface expressed FcγRIV and complement receptor 3 (CR3) on neutrophil populations. Interestingly, strain-specific levels of FcγRIV and CR3 are associated with 3F6-mIgG2a-based protection against *S. aureus*. C57BL/6J mice relied primarily on FcγR effector functions while clearance of *S.aureus* by 3F6-mIgG2a in BALB/cJ mice required complement.

Results

Generation of 3F6-mIgG mAbs. Previously, we developed mAb 3F6 that blocked interactions between the conserved surface-displayed SpA and its ligands, and protected mice against *S. aureus* bloodstream dissemination (20, 29, 30). To investigate the optimal Fc effector activity for protection in animals, we transferred the coding sequences of the variable heavy (VH) and light chains of the original 3F6 mouse hybridoma (20) onto four murine isotypes, resulting in the mAbs referred herein as 3F6-mIgG1, 3F6-mIgG2a, 3F6-mIgG2b, and 3F6-mIgG3, respectively (Fig. 1*A* and *SI Appendix*, Table S1). The corresponding antibodies were purified as visualized by Coomassie staining of sodium dodecyl sulfate–polyacrylamide gel electrophoresis (SDS–PAGE), and their identity was validated by western blotting using specific antiisotype antibodies (Fig. 1*B*). Fc N-glycosylation was documented by releasing glycans from antibody preparations and analyzed using matrix-assisted laser desorption/ionization time-of-flight mass spectrometry (*SI Appendix*, Fig. S1 *A–D*). All antibodies interacted similarly with the antigen SpA_{KKAA}, a nontoxigenic variant of SpA (Fig. 1*C*), and effectively blocked the interaction between wild-type SpA and its natural ligand, human IgG (hIgG) (Fig. 1*D* and *SI Appendix*, Table S2). The mIgG2a antibody from the original mouse hybridoma, hybrid 3F6, was included as a control.

Antibody-Mediated Protection in C57BL/6J and BALB/cJ Mice Challenged with *S. aureus*. When administered 12 h before bloodstream challenge with strain MW2, a MRSA variant,

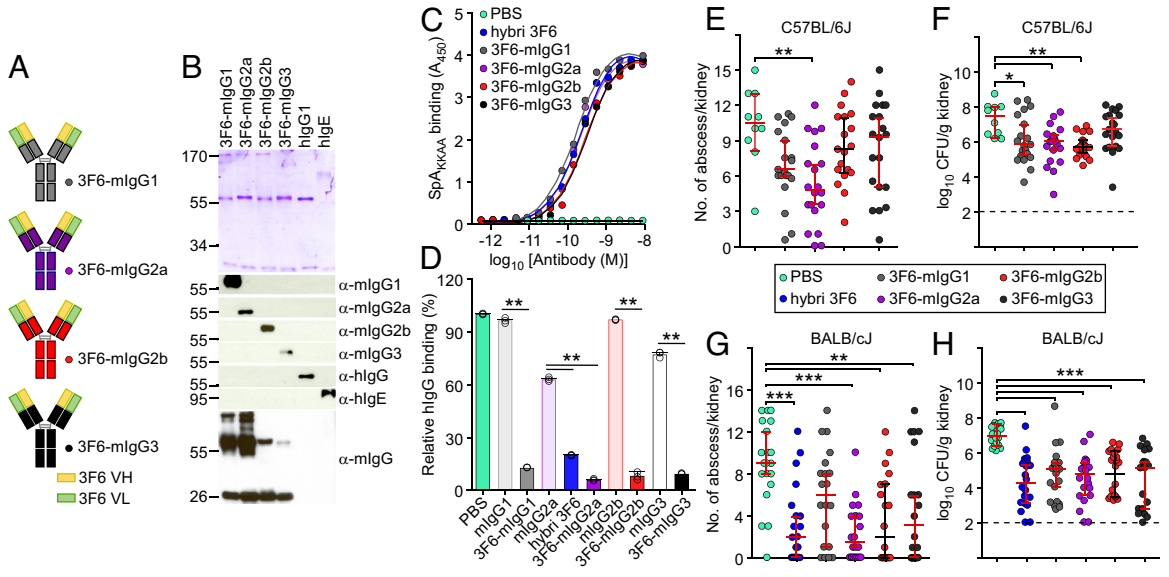

Fig. 1. Anti-*S. aureus* activity of m3F6 subclasses in C57BL/6J and BALB/cJ animals. (*A*) Schematic of recombinant mouse antibodies. (*B*) Visualization of purified antibodies using Coomassie-stained SDS–PAGE and western blotting under reducing condition. Numbers indicate masses of molecular weight markers. hIgG and hIgE were loaded as controls. (*C*) Antibody interactions with purified SpA_{KKAA} antigen assessed by ELISA (n = 3 assays); A_{450}, absorbance at 450 nm. (*D*) Recombinant mouse 3F6 antibodies prevent the association of SpA to human IgG better than isotype control antibodies. Values were normalized to SpA interaction with human IgG in Phosphate Buffered Saline (PBS) (n = 3 assays). Raw data are reported in *SI Appendix*, Table S2. (*E–H*) Enumeration of tissue surface abscesses (*E* and *G*) and bacterial loads in kidney tissues (CFU/g) (*F* and *H*) following 15-d infection with *S. aureus* MW2 of C57BL/6J (*E* and *F*) or BALB/cJ (*G* and *H*). Animals received PBS or 10 mg/kg (body weight) recombinant mouse 3F6 antibodies prior to challenge with *S. aureus*. Test antibodies are indicated on the figure. The original 3F6 mouse hybridoma (hybrid 3F6) was used as a control when indicated (*C*, *D*, *G*, and *H*). Data are presented as mean ± SEM (*C* and *D*) or medians ± 95% CIs (*E–H*) and representative of at least two independent experiments (*C* and *D*). Dashed lines (*F* and *G*) indicate the lower limit of detection. Significant differences are identified with the two-tailed Student's *t* test (*D*) and one-way ANOVA with Kruskal–Wallis test (*E–H*; ***P < 0.001; **P < 0.01; *P < 0.05). For comparison with isotype controls and animal groups see *SI Appendix*, Fig. S2 and Table S3.

3F6-mIgG variants conferred different levels of protection in animals, and the relative protection varied with the mouse strain (Fig. 1 *E*–*H* and *SI Appendix*, Fig. S2). In this infection model, bacteria disseminate from the bloodstream to organs, such as the kidneys, where they form abscesses. Clinical disease can be assessed by measuring daily weight change. On day 15 post challenge, animals are killed, and the kidneys are removed to count visible bacterial abscesses and enumerate bacterial loads by plating ground tissues (colony forming units per gram of kidney, CFU/g). In C57BL/6J mice, administration of both 3F6-mIgG1 and 3F6-mIgG2a resulted in reduced numbers of lesions (abscesses) and bacterial loads in kidneys (Fig. 1 *E* and *F* and *SI Appendix*, Fig. S2 and Table S3); protection with 3F6-mIgG2a was better than 3F6-mIgG1, in particular against weight loss (*SI Appendix*, Fig. S2*A*). Administration of 3F6-mIgG2b only resulted in the reduction of bacterial loads but not of abscesses (Fig. 1 *E* and *F* and *SI Appendix*, Fig. S2 *A*–*C* and Table S3). 3F6-mIgG3 did not provide any protection (Fig. 1 *E* and *F* and *SI Appendix*, Fig. S2 *A*–*C* and Table S3). Thus, in C57BL/6J mice, antibody protection can be ranked as 3F6-mIgG2a > 3F6-mIgG1 ≥ 3F6-mIgG2b ≫ 3F6-mIgG3 (no protection). Such a hierarchy was not observed in BALB/cJ mice. The protective activities of 3F6-mIgG1, 3F6-mIgG2a, 3F6-mIgG2b, and 3F6-mIgG3 were almost indistinguishable (Fig. 1 *G* and *H* and *SI Appendix*, Fig. S2 *D* and *E* and Table S3). We note that BALB/cJ mice harbored slightly higher numbers of lesions on the surface of kidneys (Fig. 1 *E* and *F*) and exhibited greater weight loss (vide infra, *SI Appendix*, Fig. S4 *B* and *C*) as compared with C57BL/6J animals. Nonetheless, earlier histopathology studies revealed similar architecture of abscess lesions between these mice (34–39). Thus, we rule out the possibility that the difference in 3F6 antibody activity could be caused by different pathologies. Instead, we speculate that the effector functions of crystallizable fragment (Fcγ) of mIgG subclasses or engagement with downstream receptors account for differences in protection observed in C57BL/6J mice and for strain-specific differences observed between mouse strains.

Distinct Effector Functions Promote *S. aureus* Killing in Mouse Blood. The simplest mechanism of antibody protection is neutralization whereby an antibody binds its target, for example a toxin or a virus, to block entry into host cells, and ultimately prevent intoxication or viral replication (40). Antibodies can also mark antigens on the surface of bacterial pathogens. The exposed Fc domain can then interact with Fc receptors (FcR) found on innate immune cells (41) or with the six-headed C1q molecule (42). For extracellular bacterial pathogens, both interactions may result in opsonophagocytic killing (OPK) (40). When IgG acts as the opsonin, interaction with FcγR of phagocytes promotes antibody-dependent cell-mediated phagocytosis (41, 42). When IgG and antigen form oligomeric complexes, the C1 complex is recruited via the complement component C1q (42). The classical complement pathway is initiated resulting in the coating of the bacterial cell surface with complement components such as the C3b opsonin. Complement receptors on the surface of phagocytes promote uptake of these opsonized bacteria, a process referred as complement-dependent cell-mediated phagocytosis (43). Of note, the thick envelope of *S. aureus* provides protection against direct lysis by the complement C5b-9 complex or membrane attack complex responsible for complement-dependent cytotoxicity (30, 44). To assess the opsonizing activity of 3F6 antibodies, we performed an ex vivo OPK assay by measuring the replication of *S. aureus* bacteria in freshly drawn anticoagulated mouse blood. Following 30-min incubation, sample aliquots were plated and CFU compared with the inoculum at time 0 (Fig. 2). Some samples were incubated in the

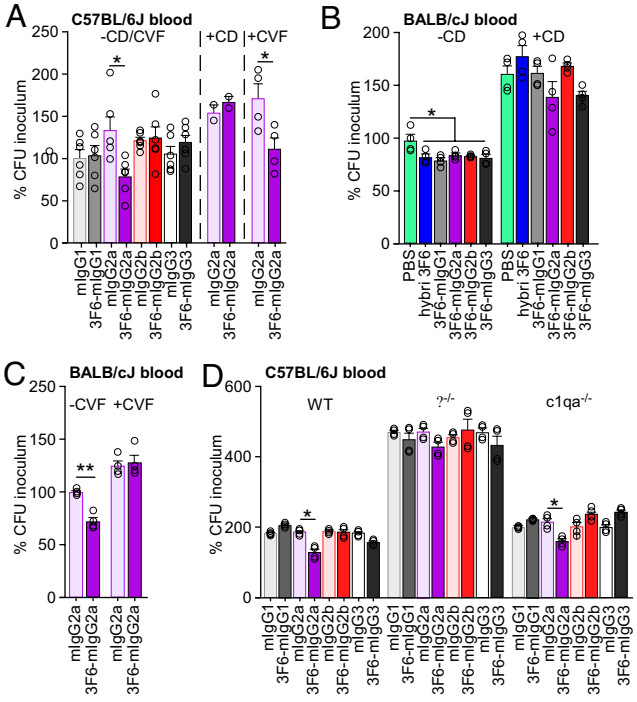

Fig. 2. OPK activity of antibodies toward *S. aureus* MW2 in anticoagulated freshly drawn blood of BALB/cJ and C57BL/6J mice. *S. aureus* MW2 survival was measured in freshly drawn (*A*) blood of C57BL/6J mice without (n = 6) or with (n = 4) cytochalasin D (−/+ CD) or cobra venom factor (−/+ CVF), (*B*) blood of BALB/cJ mice without (n = 4) or with (n = 4) cytochalasin D (−/+ CD), (*C*) blood of BALB/cJ mice without (n = 4) or with (n = 4) cobra venom factor (−/+ CVF), (*D*) blood (n = 4) of wild-type, $\gamma^{-/-}$, and *c1qa*$^{-/-}$ mice. Test antibodies (5 μg/mL blood) are indicated on the figure. Data are plotted as the average ± SEM of CFUs after 30-min incubation in blood compared with CFUs of inoculum (set as 100%). Significant differences were identified with the two-tailed Student's t test (**P < 0.01; *P < 0.05).

presence of CD, a cell-permeable inhibitor of actin polymerization that blocks phagocytosis, or cobra venom factor (CVF), a protein analogue of complement component C3 that continuously activates complement resulting in the depletion of complement activity (45) (Fig. 2 *A*–*C*). 3F6-mIgG2a was the only variant able to reduce bacterial replication in the blood of C57BL/6J mice. 3F6-mIgG2a activity was markedly reduced in the presence of CD but not in the presence of CVF, suggesting complement-independent phagocytic killing (Fig. 2*A*). When the same assay was performed with the blood of BALB/cJ mice, all 3F6 isotypes performed better than the mock control and lost their activity in the presence of CD, in agreement with a cell-mediated phagocytic process (Fig. 2*B*). To rule out the possibility that preexisting anti-*S. aureus* antibodies may have accounted for differences in bacterial replication, total CFUs of bacteria following 0- and 30-min incubation in C57BL/6J and BALB/cJ whole blood are also shown in *SI Appendix*, Fig. S3. Although C57BL/6J mice appeared to have some anti-*S. aureus* antibodies as compared with naïve BALB/cJ or μMT control mice, a correlation between preexisting antibodies and OPK activity was not observed (*SI Appendix*, Fig. S3). Since 3F6-mIgG2a conferred protection in both C57BL/6J and BALB/cJ animals and their blood (Figs. 1 and 2), this variant was further investigated. Unlike with C57BL/6J mice, pretreatment of BALB/cJ mouse blood with CVF resulted in a loss of OPK activity of 3F6-mIgG2a (Fig. 2*C*). Next, we used blood from C57BL/6J mice deficient for C1q and FcγRs. In C1q-deficient animals (C1qa$^{-/-}$), the A-chain of C1q has been deleted resulting in loss of C1q expression (46). FcγR-deficient animals ($\gamma^{-/-}$) lack the common γ-chain required for all activating receptors (FcγRI, FcγRIII, FcγRIV) (47). We found

that 3F6-mIgG2a retained its OPK activity in anticoagulated *C1qa*$^{-/-}$ blood but not in the blood of $\gamma^{-/-}$ mice (Fig. 2*D*). In conclusion, the same 3F6-mIgG2a mediates killing of *S. aureus* in complement-dependent and -independent manners in BALB/cJ and C57BL/6J mice, respectively. OPK in C57BL/6J whole blood requires the activating FcγRs.

Strain-Specific Protection against Bloodstream Dissemination in Mice Correlates with 3F6-mIgG2a Activity in Blood. To further investigate the activity of 3F6-mIgG2a, C57BL/6J WT mice and $\gamma^{-/-}$ and C1qa$^{-/-}$-deficient variants were passively immunized and challenged with *S. aureus*. As observed earlier, 3F6-mIgG2a provided protection in wild-type (WT) animals as compared with isotype control (Fig. 3 *A* and *B* and *SI Appendix*, Fig. S4*A*). 3F6-mIgG2a also provided significant protection against bacterial replication and abscess formation in C1qa$^{-/-}$ mice although disease was more pronounced as evidenced by the inability to regain weight loss (Fig. 3 *A* and *B* and *SI Appendix*, Fig. S4*A*). 3F6-mIgG2a did not afford protection in $\gamma^{-/-}$ mice (Fig. 3 *A* and *B* and *SI Appendix*, Fig. S4*A*). The data suggest that activating FcγRs are essential to effect anti-MRSA activity of antibodies in C57BL/6 mice. Deficient $\gamma^{-/-}$ and C1qa$^{-/-}$ BALB/cJ mice are not available to us. To investigate the requirement for complement, BALB/cJ and C57BL/6J mice were challenged with MRSA following passive transfer of 3F6-mIgG2a or isotype control and in the absence and presence of CVF. Of note, deletion of C1qa only affects activation of the classical (antibody-dependent) pathway while by activating the alternative pathway, C3-like CVF may lead to the complete depletion of complement (classical, lectin, alternative). As observed by others before us (48), administration of CVF resulted in acute disease in BALB/cJ animals treated with isotype control antibody, and all animals (100%) were removed from the study by day 4 post MRSA challenge while 80% survived the challenge in the control group untreated with CVF (Fig. 3*C* and *SI Appendix*, Fig. S4*B*). This experiment emphasizes the importance of the complement system as a major contributor to innate immune defenses against infection (48, 49). Weight monitoring and abscess and CFU enumerations could only be performed for surviving BALB/cJ animals and confirmed the protective activity of 3F6-mIgG2a in absence of CVF but not in its presence (Fig. 3 *E* and *F* and *SI Appendix*, Fig. S4*B*). CVF treatment was also fatal in C57BL/6J mice that received isotype control mIgG2a and were subsequently challenged with MRSA (Fig. 3*D*). However, all CVF-treated animals (100%) survived the challenge upon administration of 3F6-mIgG2a (Fig. 3*D*). Despite the high survival rate conferred by 3F6-mIgG2a, the disease was severe in absence of complement (3F6-mIgG2a + CVF) as demonstrated by the higher bacterial loads and abscess lesions and greater weight loss when compared with C57BL/6J mice that received mIgG2a and no CVF (mIgG2a – CVF) (Fig. 3 *E* and *F* and *SI Appendix*, Fig. S4*C*). Thus, the complement system is essential to control staphylococcal replication in both C57BL/6J and BALB/cJ mice but it is dispensable for the protective activity of 3F6-mIgG2a in C57BL/6J mice.

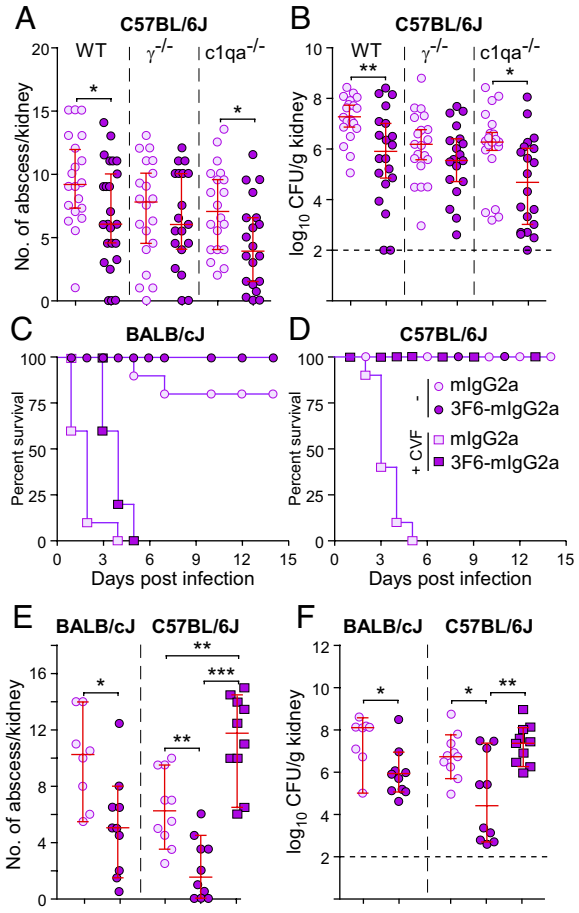

Fig. 3. 3F6-mIgG2a protects BALB/cJ and C57BL/6J mice via distinct mechanisms. (*A* and *B*) Passive immunization with 3F6-mIgG2a protects C57BL/6J WT and *c1qa*$^{-/-}$ mice but not $\gamma^{-/-}$ mice against *S. aureus* MW2 infection. mIgG2a or 3F6-mIgG2a (10 mg/kg) was given before challenge with MW2. Fifteen days post infection, kidneys (n = 20 animals, from two independent experiments) were removed to enumerate surface abscesses (*A*) and CFU (*B*). (*C*–*F*) 3F6-mIgG2a requires complement to protect BALB/cJ but not C57BL/6J mice against *S. aureus* infection. Test antibodies (10 mg/kg body weight) with or without CVF (150 μg/kg body weight) were administered to BALB/cJ (n = 7 to 10 from two independent experiments) and C57BL/6J (n = 8 to 10 from two independent experiments) mice before challenge with *S. aureus* MW2. Survival (*C* and *D*) was recorded daily, and surface abscesses (*E*) and bacterial loads (*F*) in kidneys were enumerated 15 d post infection. Data are presented as medians ± 95% CI (*A*, *B*, *E*, and *F*). Dashed lines (*B* and *F*) indicate the lower limit of detection. Significant differences were identified with the two-tailed Mann–Whitney test (*A* and *B*) or one-way ANOVA with Kruskal–Wallis test (*E* and *F*; ***P < 0.001; **P < 0.01; *P < 0.05).

Amino Acid Polymorphisms of C1q and FcγRIII Have No Impact on Antibody Activity. The distinct immune effector functions between mouse strains could be a result of genetic polymorphism of C1q and FcγRs. We used the Mouse Genome Database (MGD: http://www.informatics.jax.org) to look for amino acid substitution(s) in coding sequences and identified nonsynonymous single-nucleotide polymorphisms (nsSNPs) in the *C1qa*, *C1qb*, *C1qc*, and *Fcgr3* genes (Dataset S1) (50). *c1qa* and *c1qb* only have one nsSNP each (rs27625206 and rs13473142, respectively), *c1qc* had three nsSNPs (rs4224832, rs32277923, and rs27625239), and *fcgr3* had four nsSNPs (rs8242767, rs4222823, rs8242799, and rs8242800). We used sera from C57BL/6J or BALB/cJ mice as a source of C1q to measure interactions with 3F6-mIgG variants (Fig. 4*A* and *SI Appendix*, Table S4). As expected, 3F6-mIgG2a displayed the highest binding for C1q, but no significant difference was observed between the two sources of C1q (C57BL/6J or BALB/cJ). Similarly, C1q nsSNPs did not affect the binding of the other 3F6-mIgG subclasses (Fig. 4*A* and *SI Appendix*, Table S4). To examine the impact of FcγRIII polymorphisms, the extracellular domains of the corresponding receptor originating from BALB/cJ and C57BL/6J (with nsSNPs, rs4222823, rs8242799, and rs8242800) were produced and purified from HEK-293F cells (Fig. 4*B*). FcγRIII proteins appeared as smears on SDS–PAGE owing to N-glycosylation; the slower migration of C57BL/6J FcγRIII can be explained by glycolsylation of the NWS motif that replaces the NGR residues found in the extracellular domain of BALB/c FcγRIII (Fig. 4*B*). With the exception of 3F6-mIgG3, all

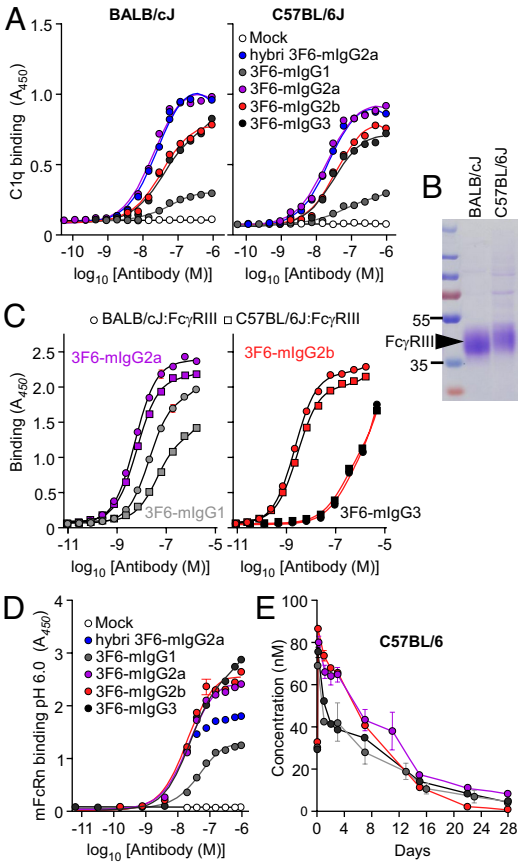

Fig. 4. Assessing the impact of C1q, FcγRIII and FcRn polymorphisms for interaction with antibodies. (*A*) Interactions between 3F6-mIgGs and C1q (n = 3 assays) were assessed using ELISA plates coated with test antibodies or mock (PBS) and incubated with BALB/cJ (*Left*) and C57BL/6J (*Right*) mouse sera. Bound C1q was detected by HRP-conjugated anti-mouse C1q. (*B*) Coomassie-stained gel of the extracellular domain of C57BL/6J and BALB/cJ FcγRIII purified from transfected HEK-293F cells. (*C*) Interactions between 3F6-mIgGs and the extracellular domain of BALB/cJ and C57BL/6J FcγRIII (n = 3 assays) were assessed using ELISA plates coated with purified FcγRIII. Bound antibodies were detected with HRP-conjugated anti-mIgG. (*D*) Interactions between 3F6-mIgGs and mFcRn (n = 3 assays) were measured at pH 6.0 using ELISA plates coated with test antibodies or mock (PBS). Bound biotinylated FcRn was detected with HRP-conjugated streptavidin. (*E*) Serum concentration over time of four 3F6-mIgGs in C57BL/6J mice (n = 5 mice per group). Absorbances (*A*, *C*, and *D*) were recorded at 450 nm (A_{450}). Data (*A*, *C*, *D*, and *E*) are presented as mean ± SEM and are representative of at least two independent experiments.

other antibodies interacted with soluble FcγRIII molecules albeit with a slightly increased affinity for the BALB/cJ FcγRIII variant; this was particularly true for 3F6-mIgG1 (Fig. 4*C* and *SI Appendix*, Table S4). Next, we wondered if the half-life of antibodies may be different in the two mouse strains. Antibody turn-over is controlled by the neonatal Fc receptor (FcRn) (51). FcRn consists of two chains encoded by the *Fcgrt* and *β2m* genes. A search in MGD did not reveal any amino acid polymorphism. Binding assays showed that 3F6-mIgG2a, 3F6-mIgG2b, and 3F6-mIgG3 had similar affinity for mouse FcRn at pH 6.0 (Fig. 4*D* and *SI Appendix*, Table S4). In C57BL/6J mice, a half-life of 5, 9, 6.5, and 4.5 d were measured, respectively, for m3F6-IgG1, 3F6-mIgG2a, 3F6-mIgG2b, and 3F6-mIgG3 (Fig. 4*E*). Although the higher half-life of 3F6-mIgG2a can contribute to protection in C57BL/6J mice, the half-life alone cannot account for the protective effect of 3F6-mIgG1 (4.5 d) over 3F6-mIgG3 (5 d) observed upon challenge with MRSA (Fig. 1 *E* and *F*). Altogether, these data rule out the possibility that differences in *C1qa*, *C1qb*, *C1qc*, and *Fcgr3* genes or in antibody half-life account for isotype-dependent and mouse strain-dependent activity of 3F6-mIgGs.

Neutrophils of C57BL/6J and BALB/cJ Mice Display Different Levels of FcγRIV and CR. The MGD analysis revealed additional SNPs in introns and other untranslated regions of FcγR and complement genes that could result in differential expression and thus impact the activity of 3F6-mIgGs (Datasets S1 and S2). However, the number of SNPs was too large to explore directly. Instead, we decided to compare the relative abundance of FcγRs and CR3 and complement receptor 4 (CR4) on neutrophils of C57BL/6J and BALB/cJ mice. Neutrophils are critical to fight *S. aureus* infections (52). Animals were inoculated intravenously with mock (naïve control) or *S. aureus* and killed on days 1, 5, 10, or 15. Side-by-side comparisons of CFU and abscesses in blood and kidneys did not reveal any significant differences between infected C57BL/6J and BALB/cJ mice over time (*SI Appendix*, Fig. S5 *A–C*). Positive $CD11b^+Ly6G^+$ selections were used to sort (*SI Appendix*, Fig. S5*D*) and enumerate neutrophils over the course of infection (*SI Appendix*, Fig. S5*E*). The $CD11b^+Ly6G^+$ cell count was higher in uninfected BALB/cJ mice as compared with C57BL/6J mice. However, this difference disappeared following infection which resulted in a dramatic increase in $CD11b^+Ly6G^+$ cell counts starting on day 5 (*SI Appendix*, Fig. S5*E*). Individual levels of surface FcγRs and CRs were also assessed by immune-staining and measuring relative fluorescence intensities (Fig. 5 *A–F*). Uninfected BALB/cJ mice always produced more FcγRI than any other groups, and infection resulted in reduction of the FcγRI signal with no statistical difference between mouse strains (Fig. 5*A*). Surface display of FcγRIIb remained essentially the same over the course of infection with levels similar between mouse strains (Fig. 5*B*). In general, neutrophils of BALB/cJ mice displayed relatively more FcγRIII, CR3, and CR4 than those of C57BL/6J mice (Fig. 5 *C*, *E*, and *F*). Conversely, relative levels of FcγRIV were significantly higher in neutrophils of C57BL/6J mice compared with BALB/cJ mice (Fig. 5*D*). The overall levels of CR4 were unchanged following MRSA challenge, but levels of FcγRIII, FcγRIV, and CR3 increased significantly in neutrophils of both C57BL/6J and BALB/cJ animals over the course of infection (Fig. 5 *C–E*). Notably, relative FcγRIV levels were higher in neutrophils of C57BL/6J mice while CR3 levels were higher in neutrophils of BALB/cJ animals (Fig. 5 *D* and *E*). The opsonin iC3b generated upon cleavage of complement protein C3 is a major ligand of CR3 (43). We observed that C3 levels were similar between the two mouse strains in uninfected serum samples but increased significantly on days 5 and 10 post MRSA infection; infection in BALB/cJ mice resulted in even higher C3 increases as compared with C57BL/6J mice (Fig. 5*G*). Together, these data point to specific roles for FcγRIV and CR3 in C57BL/6J and BALB/cJ animals, respectively, that may be the basis for the different effector function of 3F6-mIgG2a observed in these animals during *S. aureus* infection.

3F6-mIgG2a Protection Requires FcγRIV in C57BL/6J and CR3 in BALB/cJ Mice. To explore the requirement of specific immune receptors for 3F6-mIgG2a-mediated protection in different mouse strains, we employed blocking antibodies against FcγRIV (α-FcγRIV, 9E9) and CR3 (α-CD11b, M1/70) (47, 53, 54). First, α-FcγRIV and α-CD11b were treated with peptide-N-glycosidase F (PNGase F) to remove N-linked oligosaccharides and eliminate the Fc-mediated effector functions of these antibodies. Successful deglycosylation and loss of Fc-mediated functions were documented by the faster mobility of antibodies on SDS–PAGE (*SI Appendix*, Fig. S6*A*) and their inability to deplete circulating $CD11b^+Ly6G^+$ following injection in animals for 1, 5, and 14 d (*SI Appendix*, Fig. S6*B*). These blocking antibodies remained bound on the surface of circulating neutrophils for at least 5 d

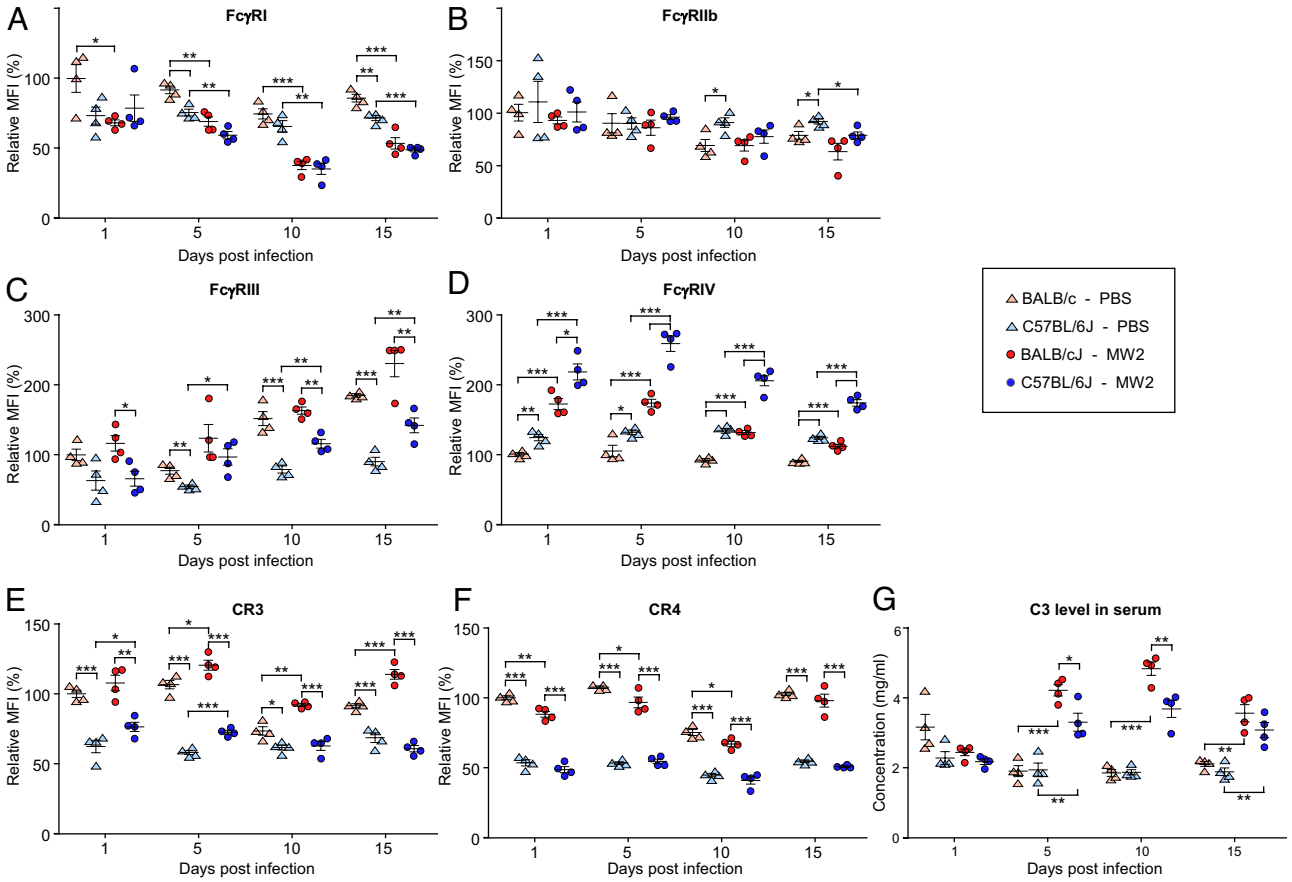

Fig. 5. Relative levels of FcγRs and CRs in naïve and infected BALB/cJ and C57BL/6J mice. Animals that had received PBS or *S. aureus* MW2 (shown in *SI Appendix*, Fig. S5 *A*–*C*) were euthanized on day 1, 5, 10, or 15 post infection. Flow cytometry was used to gate for $CD11b^{+}Ly6G^{+}$ neutrophils (scheme shown in *SI Appendix*, Fig. S5*D*) that were subsequently stained with fluorescently labeled anti-FcγRI (*A*), -FcγRIIb (*B*), -FcγRIII (*C*), -FcγRIV (*D*), CR3 (*E*), and CR4 (*F*) antibodies. The fluorescence intensity of each receptor resulted in only one peak. As a result, the median fluorescence intensity (MFI) was used to represent the level of these receptors. 100% corresponds to the MFI measured for each receptor in the mock (PBS) BALB/cJ samples at day one. (*G*) Levels of complement component C3 in sera from naïve and infected BALB/cJ and C57BL/6J mice. Data are presented as mean ± SEM. Significant differences were identified with the two-way ANOVA with the Tukey test (***$P < 0.001$; **$P < 0.01$; *$P < 0.05$).

after injection, as demonstrated by their ability to compete for staining using fluorescently labeled α-CR3 (*SI Appendix*, Fig. S6*C*) and α-FcγRIV (*SI Appendix*, Fig. S6*D*). Thus, PNGase F-treated α-FcγRIV and α-CD11b can be used to selectively block the access to the FcγRIV and CR3 receptors without depleting neutrophil counts in vivo. These antibodies were administered to groups of BALB/cJ and C57BL/6J animals along with a mock control; animals also received the control and test antibodies, mIgG2a and 3F6-mIgG2a, respectively. All animals were challenged with MRSA for 5 d (Fig. 6 *A* and *B*). The administration of α-CD11b, but not of α-FcγRIV, abrogated 3F6-mIgG2a protection in BALB/cJ mice (Fig. 6*A*). In contrast, protection afforded by 3F6-mIgG2a in C57BL/6J mice was eliminated in the presence of blocking α-FcγRIV, but not, α-CD11b antibodies (Fig. 6*B*). Thus, expression patterns of FcγRs and CRs on immune cells govern antibody-mediated protective functions. This finding implies that the same therapeutic antibody may function via distinct mechanisms in different hosts.

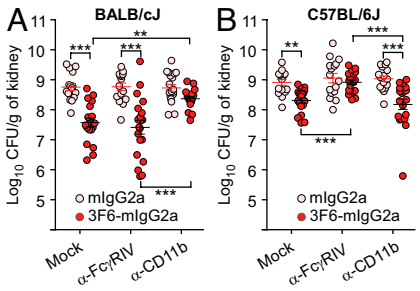

Fig. 6. Impact of FcγRIV and CR3 (CD11b) blocking antibodies on the activity of 3F6-mIgG2a in animals challenged with *S. aureus*. (*A* and *B*) Enumeration of bacterial loads in kidneys from *S. aureus* MW2-infected BALB/cJ (*A*) or C57BL/6J (*B*) mice. Animals (n = 16 to 20 animals, from two independent experiments) received 3F6-mIgG2a or isotype control mIgG2a (10 mg/kg of body weight) and deglycosylated α-FcγRIV or α-CD11b (CR3) (7.5 mg/kg of body weight) as indicated, before challenge with *S. aureus* MW2. Bacterial loads in kidneys were enumerated at 5 d post infection. Data are presented as mean ± SEM. Significant differences were identified with the two-tailed Student's t test (***$P < 0.001$; **$P < 0.01$).

Discussion

Complementarity-determining region of IgG initiates the recognition of antigens, and IgG-Fcγ mediates downstream effector functions by interacting with FcγRs and complement component C1q. Even neutralizing antibodies, that primarily interfere with toxin binding or virus entry into target cells, display different efficacies depending on their subclass (55–57). For example, the mAb 19D9 that binds the protective antigen of *Bacillus anthracis* toxins displays greater neutralization when produced as a mouse IgG2a variant; when tested in mice, this protection was found to require FcγRs (56). In mice, FcγRI, FcγRIII, and FcγRIV operate as activating receptors and FcγRIIb as an inhibitory receptor

(33, 47, 58). Using soluble FcγRs, it was found that each receptor interacts with different affinity with each IgG subclass. mIgG2a and mIgG2b interact with all FcγRs, mIgG1 interacts only with FcγRIII and FcγRIIb, and mIgG3 only binds FcγRI weakly (41, 47). The sum of both activating and inhibitory signals triggered through immune complex binding to FcγRs determines the outcome of immune responses (33, 58). When measured as an activating-to-inhibitory (A/I) ratio, the highest values were reported for mIgG2a followed by mIgG2b suggesting that these two subclasses should be quite potent in vivo; conversely mIgG1 that interacts more strongly with inhibitory FcγRIIB than FcγRIII displays the least activating activity (58). Other factors such as valency, avidity, glycosylation, abundance, and distribution on immune cells also modulate IgG activity, a complexity that can be extrapolated using mathematical models (59) or investigated using antibody engineering and knockout animals that lack distinct effectors of IgGs (41). Antibodies also interact with different affinities with C1q following the hierarchy mIgG2a > mIgG2b ≥ mIgG3 > mIgG1 (32).

Earlier, we characterized 3F6-hIgG1 in a BALB/cJ mouse model of staphylococcal bloodstream dissemination. Of note, hIgG1 is considered to be the equivalent of mIgG2a. We found that N297-linked glycosylation of Fcγ, specifically fucosyl mono- and di-galactosyl (G1F/G2F) substitutions were essential for complement-mediated protection of animals (30). However, removal of fucosyl residues that abrogated C1q binding but enhanced binding toward activating FcγRs, also protected animals from *S. aureus* bloodstream challenge (30). To better delineate the role of Fcγ function for *S. aureus* uptake and killing in mice, we generated the four mouse variants 3F6-mIgG1, 3F6-mIgG2a, 3F6-mIgG2b, and 3F6-mIgG3. Here, we find that the activity of antibodies varies depending on the subclass and mouse strain. The latter finding was unexpected. 3F6-mIgG2a protected BALB/cJ from *S. aureus* bloodstream challenge in a complement-dependent and FcγRIV-independent manner. Conversely, 3F6-mIgG2a reduced bacterial replication in C57BL/6J mice in an FcγRIV-dependent and complement-independent manner. These conclusions were reached by passively immunizing wild-type animals following chemical depletion of complement (CVF), and immunological neutralization of FcγRIV and CR3 or by exploiting knockout *C1qa*$^{-/-}$ and $\gamma^{-/-}$ C57BL/6J mice. A similar conclusion was reached when measuring bacterial replication in anticoagulated whole blood from these animals. Other surprising results included protection mediated by 3F6-mIgG3 in BALB/cJ but not C57BL/6J mice, a protection that was negated upon CVF pretreatment, and protection mediated by 3F6-mIgG1 in both animals, in spite of a low A/I ratio and low affinity for C1q. We suspect that 3F6-mIgG3 protection in BALB/cJ mice is the result of augmented C1q recruitment. With respect to 3F6-mIgG1, we suspect that the abundance of SpA and the fact that each SpA molecule can be labeled with five 3F6 molecules on the bacterial surface are sufficient to compensate for weak C1q and FcγRs interactions; further SpA does not interact with mIgG1-Fcγ and thus cannot block the effector functions of this subclass (31, 60). However, how can we account for the distinct activities of the same antibody, 3F6-mIgG2a, in two mouse strains? We explored the possibility of nucleotide polymorphisms (50, 61). Little is known about SNPs affecting antibody-based immunotherapy in mouse models, unlike the better characterized polymorphisms of human FcγRs, FcRn, and complement encoding genes (62–65). A missense mutation that impairs the inhibitory function of (human) hFcγRIIb and two SNPs in the promoter of the gene result in increased expression of this receptor in several types of immune cell (62, 66). A phenylalanine to valine substitution at position 158 increases the affinity of hFcγRIIIA for hIgG1, hIgG2, and hIgG3 (67). A variable number of tandem repeats within the *hFcRn* promoter influences its transcription and response to antibody therapy (68–70). Polymorphisms in complement-encoding genes have also been linked to the clinical response of patients receiving antibody therapies (71, 72). Based on these observations, we explored the possibility that nsSNPs in the coding sequences of the *C1qa*, *C1qb*, *C1qc*, and *Fcgr3* genes could account for the difference in 3F6-mIgG2a activity. However, this line of investigation was not met with success. Of note, we did not identify SNPs in the *Fcgrt* and *β2m* coding segments of the two strains. SNPs in noncoding (untranslated) sequences can also affect the expression of genes. Mutations that could have affected the expression of the *Fcgrt* and *β2m* genes were ruled out by measuring the half-life of all four antibody subclasses in BALB/cJ and C57BL/6J mice. Next, we asked if mutations may have affected the expression levels of Fcγ and complement receptor genes. Here, we focused our analysis on neutrophils as they represent the first line of defense against *S. aureus* bacteria (52). Neutrophils of naïve BALB/cJ and C57BL/6J mice were found to express different patterns of FcγRIII, FcγRIV, CR3, and CR4. Importantly, the relative ratio of FcγRIV over CR3 was found to be higher on neutrophils of C57BL/6J mice as compared to neutrophils of BALB/cJ mice. This skewed FcγRIV/CR3 ratio was maintained when animals were challenged with *S. aureus* and offers a molecular basis for the distinct opsonophagocytic activity of 3F6-mIgG2a in the two strains. We conclude that noncoding genetic differences can modulate the downstream effector capacity of immune responses and govern the protective mechanisms of antibody. We speculate that this is not restricted to laboratory animals. In fact, a recent study that examined the relative abundance of FcγRs on human leukocytes found a dichotomy between donors with either low- or high-expression levels of inhibitory hFcγRIIb (73). Thus, each IgG subclass may exert protection via different mechanisms in distinct hosts. One explanation is that genetic polymorphisms between hosts may result in distinct distribution and relative abundance of complement and Fcγ receptors on immune cell populations.

Materials and Methods

Ethics Statement. Animal research was performed in accordance with institutional guidelines following experimental protocol review, approval, and supervision by the Institutional Animal Care and Use Committee at The University of Chicago. Experiments with *S. aureus* were performed in biosafety level 2 (BSL2)/animal BSL2 containment upon review by The University of Chicago Institutional Biosafety Committee.

Bacterial Strain, Mammalian Cell Line and Growth Media. Community-associated MRSA USA400 (MW2) was grown in tryptic soy broth (TSB) at 37 °C. Suspension serum-free adapted FreeStyle™ 293-F cells were cultured in FreeStyle™ 293 Expression Medium (Life Technologies) and maintained in a 5% CO_2 humidified incubator at 37 °C.

Construction, Expression, and Purification of Recombinant 3F6-mIgGs. The constant heavy chains of mIgG1 (Uniprot No. P01868), mIgG2a (Uniprot No. P01863), mIgG2b (Uniprot No. A0A075B5P3), and mIgG3 (Uniprot No. P03987-2) were assembled with VH chain of the mouse hybridoma mAb 3F6 (20) resulting in 3F6-mIgG1, 3F6-mIgG2a, 3F6-mIgG2b, and 3F6-mIgG3. The light chain was identical in all mouse 3F6 antibodies. The corresponding amino acid sequences are shown in *SI Appendix*, Table S1. The genes encoding these antibodies were synthesized by Integrated DNA Technologies, Inc., and polymerase incomplete primer extension was used to swap the gene constructs into the expression vector pVITRO1-102.1F10-IgG1/λ (Addgene, number 50366) (74) as described earlier (29). All plasmids were sequenced and transfected into FreeStyle™ 293-F cells using polyethylenimine (75). Transfectants were isolated with hygromycin B (400 μg/mL) selection and expanded in TripleFlask Cell Culture Flasks (ThermoFischer). Antibodies were affinity purified from supernatants of expanded cultures over

protein G-sepharose (Genscript), dialyzed against Phosphate Buffered Saline (PBS) as described (30) and visualized by separation on 12% SDS–PAGE. For immunoblotting, proteins on SDS–PAGE were transferred to nitrocellulose membranes and probed with HRP-conjugated anti-mIgG1 (Fisher Scientific), -mIgG2a (Fisher Scientific), -mIgG2b (Fisher Scientific), -mIgG3 (Fisher Scientific), -mIgG (Cell Signaling), -hIgG (Bio-rad), and hIgE (ThermoFisher).

Construction, Expression, and Purification of Recombinant mFcγRIII. The plasmid pCMV3-SP-N-His-Mouse CD16/FCGR3 harboring full-length cDNA of BALB/cJ FcγRIII was purchased from SinoBiological (MG50326-NH) and served as a template for further mutagenesis. Primers 5′GTCTGGTACCACACTTGAATCTAGAGCGGCCGCCGAATT3′ and 5′GCCGCTCTAGATTCAAGTGTGGTACCAGACTAGAGA3′ were used to delete the transmembrane and cytoplasmic domains of BALB/cJ FcγRIII. The plasmid harboring only the extracellular domain of BALB/cJ FcγRIII served as a template to introduce three amino acids found in the extracellular domain of C57BL/6J FcγRIII using primers 5′TGGTCATCCATCCGGAGCCAGGTCCAAAGTAGTTACACGTTTAAGGCCAC3′ and 5′ACTTTGGACCTGGCTCCGGATGGATGACCAGTTGTGGAACCACTGGGTAGAA3′. The plasmids encoding the extracellular domain of BALB/cJ FcγRIII or C57BL/6J FcγRIII were transiently transfected into FreeStyle™ 293-F cells using polyethylenimine. Culture supernatants were collected and subjected to Ni-NTA column to purify the extracellular domain of BALB/cJ FcγRIII and C57BL/6J FcγRIII.

Enzyme-Linked Immunosorbent Assay. Binding measurements to SpA_{KKAA} were performed in microtiter plates (Nunc Maxisorp) coated with 1 μg/mL SpA_{KKAA} in 0.1 M carbonate buffer (pH 9.5) at 4 °C overnight. Wells were blocked before incubation with serial concentrations of recombinant 3F6-mIgGs. To measure inhibition of SpA binding to hIgG, microtiter plates were coated overnight with 10 μg/mL SpA and then blocked for 1 h. Next, plates were incubated with PBS or 200 μg/mL isotype control antibodies (mIgG1, mIgG2a, mIgG2b, or mIgG3, Fisher Scientific) or 3F6-mIgGs prior to incubation with HRP–conjugated hIgG (1 μg/mL, Jackson ImmunoResearch). To measure binding to mouse C1q or mouse neonatal Fc receptor (mFcRn), microtiter plates were coated with serial dilutions of purified 3F6-mIgGs overnight. After blocking, wells were incubated as indicated for 2 h at room temperature with 100 μL wild-type C57BL/6J or BALB/cJ mouse sera followed by incubation with HRP-conjugated anti-C1q antibody (Bio-rad) or wells were incubated for 2 h at pH 6.0 with biotinylated mFcRn (2 μg/mL, Immunitrack) prior to incubation with HRP-conjugated streptavidin (4 μg/mL, New England Biolabs). To measure binding to the extracellular domain of C57BL/6J and BALB/cJ FcγRIII, microtiter plates were coated with 10 μg/mL of the purified receptors at 4 °C overnight. Wells were blocked before incubation with serial concentrations of recombinant 3F6-mIgGs, followed by incubation with HRP-conjugated anti-mIgG (Cell Signaling). To measure the concentration of complement component C3, mouse sera were diluted 31,250-fold in PBS before coating microtiter plates at 4 °C overnight. Wells were blocked before incubation with the Goat anti-mouse C3 (CompTech). Serum C3 concentrations were calculated using a standard curve of mouse C3 (CompTech) diluted in PBS at a range of 0 to 5 μg/mL. All plates were developed using OptEIA reagent (BD Biosciences). Experiments were performed in triplicate to calculate averages and SE of the mean and repeated for reproducibility.

***S. aureus* Replication in Whole Blood.** To measure staphylococcal survival in vitro, PBS, isotype control antibodies (mIgG1, mIgG2a, mIgG2b, or mIgG3), or 3F6-mIgGs were mixed in a 50-μL suspension containing 2.5×10^5 CFU of strain USA400 (MW2) and added to 0.5 mL freshly drawn mouse blood. Blood was anticoagulated with 5 μg/mL desirudin and, where indicated, preincubated for 10 min with cytochalasin D (CD, Invitrogen) or 20 min with CVF (Comptech). After incubation with bacteria at 37 °C for 0 or 30 min, 0.5 mL SK Buffer (PBS containing 0.5% saponin, 100 U streptokinase, 50 μg trypsin, 1 μg DNase, and 5 μg RNase) was added to each sample for 10 min at 37 °C prior to plating on agar for CFU enumeration. This step was performed to liberate bacteria from fibrin agglutinates (76). Assays were performed in duplicate and repeated for reproducibility.

Animal Infection. C57BL/6J and BALB/cJ mice (6 to 7 wk of age) were obtained from Jackson Laboratory. Mating pairs of $C1qa^{-/-}$ (46) and $\gamma^{-/-}$ (47) animals in the C57BL/6J background were kindly provided by Michael Diamond from Washington University and bred in our animal facility. For passive immunization studies, animals were injected into the peritoneum with 10 mg/kg of indicated antibody 16 to 24 h before challenge. When indicated, animals were simultaneously injected with CVF (0.75 mg/kg), α-CD11b (7.5 mg/kg), or α-FcγRIV (7.5 mg/kg). For challenge with *S. aureus*, animals were anesthetized with a cocktail of ketamine-xylazine (50 to 65 and 3 to 6 mg/kg). Cultures of USA400 (MW2) were grown to an absorbance at 600 nm of 0.42, and bacteria were washed in PBS once and adjusted to a suspension of 6.5×10^7 CFU/ml. 100 μL of this suspension was injected into the periorbital venous plexus of anesthetized animals. Animals were monitored for survival and clinical signs of disease, and body weight recorded daily. When indicated, mice were killed on day 1, 5, 10, or 15 post infection by carbon dioxide inhalation. Blood, serum, and kidneys tissues were collected and suspended in SK Buffer before plating serial dilution for CFU enumerations. Kidney abscesses were reported by visible enumeration. Animal experiments were repeated at least once.

Flow Cytometry Analysis. Blood samples (100 μL) from naïve or challenged mice were treated with RBC lysis buffer (Biolegend), centrifuged (350 × g) and supernatants discarded. Cells in pellets were washed in cold PBS and resuspended in PBS with 5% BSA for staining with anti-CD11b-APC/Cy7 (Biolegend), anti-Ly6G-BV650 (Biolegend), anti-FcγRI-PerCPCy5.5 (Biolegend), anti-FcγRIIb-PE (Biolegend), anti-FcγRIII-PE/Cy7 (Biolegend), anti-FcγRIV-FITC (Biolegend), and anti-CD11c-APC (Biolegend) antibodies in the dark and on ice for 30 min. All stained samples were analyzed using a flow cytometer (BD LSRII 3-8, BD Biosciences). Total neutrophils were obtained by gating $CD11b^+Ly6G^+$ cells. The fluorescence intensity of each receptor in neutrophils resulted in a single peak, thus the median fluorescence intensity (MFI) was used to represent the level of these receptors. 100% was set as the MFI data recorded for each receptor from PBS-treated BALB/cJ mice. Experiments were performed at least twice.

In Vivo Half-Life of Recombinant 3F6-mIgGs. To measure antibody pharmacokinetics and dynamics, mice were injected into the peritoneal cavity with antibodies (10 mg/kg body weight). After 1 and 6 h as well as 1, 2, 3, 7, 11, 15, 22, and 28 d, blood was sampled from the retroorbital plexus and sera were analyzed by enzyme-linked immunosorbent assay (ELISA). Plasma antibody concentrations were calculated using a standard curve of 3F6-mIgGs diluted into mouse plasma at a range of 1 to 500 ng/mL. Antibody half-life was calculated using $N(t) = N_0\,(1/2)^{t/t1/2}$, where N_0 is the highest concentration of 3F6-mIgGs, N(t) is the nondecayed concentration at time t, and $t_{1/2}$ is the half-life of the decaying concentration. Experiments were performed at least twice.

Removal of N-Glycosyl Groups from Blocking Antibodies. Blocking antibody against CD11b or FcγRIV (α-CD11b or α-FcγRIV) in PBS without sodium azide were purchased from Biolegend. 75 μL PNGase F (New England Biolabs, P0704L) was added to 5 mg α-CD11b or α- FcγRIV at 37 °C for 4 h. The antibodies were repurified over protein G-sepharose (Genscript).

Statistical Analysis. Staphylococcal survival in blood and ELISA data were analyzed with the two-tailed Student's *t* test. Bacterial loads and abscess numbers in renal tissues were analyzed with the two-tailed Mann–Whitney test or one-way ANOVA with Kruskal–Wallis test. When indicated, the lower limit of detection was determined by mixing a known concentration of bacteria with a known weight of uninfected tissue or blood. Two-way repeated measure ANOVA with Bonferroni's multiple comparisons test was used to analyze changes in body weight. Percentage of neutrophil and MFI data were analyzed using two-way ANOVA with the Tukey test. All data were analyzed by Prism (GraphPad Software, Inc., La Jolla USA), and statistical significance was indicated as follows: *, $P < 0.05$; **, $P < 0.01$; ***, $P < 0.001$.

Data, Materials, and Software Availability. All study data are included in the article and/or *SI Appendix*.

ACKNOWLEDGMENTS. We thank Vilasack Thammavongsa for carefully reading the manuscript and for thoughtful comments, and members of our laboratory for discussion. This project was supported by funds from the National Institute of Allergy and Infectious Diseases, NIH under award AI148543.

Author affiliations: [a]Department of Microbiology, Howard Taylor Ricketts Laboratory, The University of Chicago, Lemont, IL 60439; [b]Institute of Infectious Diseases, Shenzhen Bay Laboratory, Shenzhen 518132, China; and [c]Department of Chemistry and Biochemistry, University of Maryland, College Park, MD 20742

Author contributions: X.C., O.S., and D.M. designed research; X.C., H.G., T.P., C.O., and M.G. performed research; X.C., L.-X.W., and D.M. analyzed data; and X.C. and D.M. wrote the paper.

1. F. D. Lowy, *Staphylococcus aureus* infections. *New Engl. J. Med.* **339**, 520–532 (1998).
2. S. Y. Tong, J. S. Davis, E. Eichenberger, T. L. Holland, V. G. Fowler Jr., *Staphylococcus aureus* infections: Epidemiology, pathophysiology, clinical manifestations, and management. *Clin. Microbiol. Rev.* **28**, 603–661 (2015).
3. M. Z. David, R. S. Daum, Community-associated methicillin-resistant *Staphylococcus aureus*: Epidemiology and clinical consequences of an emerging epidemic. *Clin. Microbiol. Rev.* **23**, 616–687 (2010).
4. H. F. Wertheim *et al.*, Risk and outcome of nosocomial *Staphylococcus aureus* bacteraemia in nasal carriers versus non-carriers. *Lancet* **364**, 703–705 (2004).
5. L. Thomer, O. Schneewind, D. Missiakas, Pathogenesis of *Staphylococcus aureus* bloodstream infections. *Annu. Rev. Pathol.* **11**, 343–364 (2016).
6. H. S. Ammerlaan, J. A. Kluytmans, H. F. Wertheim, J. L. Nouwen, M. J. Bonten, Eradication of methicillin-resistant Staphylococcus aureus carriage: A systematic review. *Clin. Infect. Dis.* **48**, 922–930 (2009).
7. F. R. DeLeo, M. Otto, B. N. Kreiswirth, H. F. Chambers, Community-associated meticillin-resistant Staphylococcus aureus. *Lancet* **375**, 1557–1568 (2010).
8. L. Czaplewski *et al.*, Alternatives to antibiotics-a pipeline portfolio review. *Lancet Infect. Dis.* **16**, 239–251 (2016).
9. J. T. Poolman, Expanding the role of bacterial vaccines into life-course vaccination strategies and prevention of antimicrobial-resistant infections. *NPJ Vaccines* **5**, 84 (2020).
10. V. G. Fowler Jr., R. A. Proctor, Where does a Staphylococcus aureus vaccine stand? *Clin. Microbiol. Infect.* **20** (suppl. 5), 66–75 (2014).
11. D. Missiakas, O. Schneewind, *Staphylococcus aureus* vaccines: Deviating from the carol. *J. Exp. Med.* **231**, 1645–1653 (2016).
12. M. J. Kuehnert *et al.*, Prevalence of Staphylococcus aureus nasal colonization in the United States, 2001–2002. *J. Infect. Dis.* **193**, 172–179 (2006).
13. A. Lebon *et al.*, Dynamics and determinants of Staphylococcus aureus carriage in infancy: The generation R study. *J. Clin. Microbiol.* **46**, 3517–3521 (2008).
14. Y. Si *et al.*, Inhibition of protective immunity against Staphylococcus aureus infection by MHC-restricted immunodominance is overcome by vaccination. *Sci. Adv.* **6**, eaaw7713 (2020).
15. C.-M. Tsai *et al.*, Non-protective immune imprint underlies failure of Staphylococcus aureus IsdB vaccine. *Cell Host Microbe.* **30**, 1163–1172.e6 (2022).
16. C.-M. Tsai, I. A. Hajam, J. Caldera, G. Y. Liu, Integrating complex host-pathogen immune environments into S. aureus vaccine studies. *Cell Chem. Biol.* **29**, 730–740 (2022).
17. F. Falugi, H. K. Kim, D. M. Missiakas, O. Schneewind, The role of protein A in the evasion of host adaptive immune responses by *Staphylococcus aureus*. *mBio* **4**, e00575-13 (2013).
18. A. Forsgren, J. Sjoquist, "Protein A" from S. aureus. I. Pseudo-immune reaction with human gamma-globulin. *J. Immunol.* **97**, 822–827 (1966).
19. A. Forsgren, P. G. Quie, Effects of staphylococcal protein A on heat labile opsonins. *J. Immunol.* **112**, 1177–1180 (1974).
20. H. K. Kim *et al.*, Protein A-specific monoclonal antibodies and the prevention of *Staphylococcus aureus* disease in mice. *Infect. Immun.* **80**, 3460–3470 (2012).
21. A. R. Cruz *et al.*, Staphylococcal protein A inhibits complement activation by interfering with IgG hexamer formation. *Proc. Natl. Acad. Sci. U.S.A.* **118**, e2016772118 (2021).
22. E. H. Sasso, G. J. Silverman, M. Mannik, Human IgM molecules that bind staphylococcal protein A contain VHIII H chains. *J. Immunol.* **142**, 2778–2783 (1989).
23. N. T. Pauli *et al.*, Staphylococcus aureus infection induces protein A–mediated immune evasion in humans. *J. Exp. Med.* **211**, 2331–2339 (2014).
24. H. K. Kim, F. Falugi, D. M. Missiakas, O. Schneewind, Peptidoglycan-linked protein A promotes T cell-dependent antibody expansion during Staphylococcus aureus infection. *Proc. Natl. Acad. Sci. U.S.A.* **113**, 5718–5723 (2016).
25. E. E. Radke *et al.*, Diversity of functionally distinct clonal sets of human conventional memory B cells that bind Staphylococcal protein A. *Front. Immunol.* **12**, 662782 (2021).
26. M. Shi, S. E. Willing, H. K. Kim, O. Schneewind, D. Missiakas, Peptidoglycan contribution to the B cell superantigen activity of Staphylococcal protein A. *mBio* **12**, e00039-21 (2021).
27. H. K. Kim, A. G. Cheng, H.-Y. Kim, D. M. Missiakas, O. Schneewind, Non-toxigenic protein A vaccine for methicillin-resistant *Staphylococcus aureus* infections. *J. Exp. Med.* **207**, 1863–1870 (2010).
28. M. Shi *et al.*, A protein A based Staphylococcus aureus vaccine with improved safety. *Vaccine* **39**, 3907–3915 (2021).
29. X. Chen, Y. Sun, D. Missiakas, O. Schneewind, Staphylococcus aureus decolonization of mice with monoclonal antibody neutralizing protein A. *J. Infect. Dis.* **219**, 884–888 (2019).
30. X. Chen *et al.*, Glycosylation-dependent opsonophagocytic activity of staphylococcal protein A antibodies. *Proc. Natl. Acad. Sci. U.S.A.* **117**, 22992–23000 (2020).
31. X. Chen, O. Schneewind, D. Missiakas, Engineered human antibodies for the opsonization and killing of Staphylococcus aureus. *Proc. Natl. Acad. Sci. U.S.A.* **119**, e2114478119 (2022).
32. J. M. Chemouny *et al.*, Protective role of mouse IgG1 in cryoglobulinaemia; insights from an animal model and relevance to human pathology. *Nephrol. Dialysis. Trans.* **31**, 1235–1242 (2016).
33. F. Nimmerjahn, J. V. Ravetch, Fcgamma receptors: Old friends and new family members. *Immunity* **24**, 19–28 (2006).
34. J. Bubeck Wardenburg, W. A. Williams, D. Missiakas, Host defenses against *Staphylococcus aureus* infection require recognition of bacterial lipoproteins. *Proc. Nat. Acad. Sci. U.S.A.* **103**, 13831–13836 (2006).
35. A. G. Cheng *et al.*, Genetic requirements for *Staphylococcus aureus* abscess formation and persistence in host tissues. *FASEB J.* **23**, 3393–3404 (2009).
36. H. K. Kim, H. Y. Kim, O. Schneewind, D. M. Missiakas, Identifying protective antigens of *Staphylococcus aureus*, a pathogen that suppresses host immune responses. *FASEB J.* **25**, 3605–3612 (2011).
37. V. Thammavongsa, D. M. Missiakas, O. Schneewind, *Staphylococcus aureus* conversion of neutrophil extracellular traps into deoxyadenosine promotes immune cell death. *Science* **342**, 863–866 (2013).
38. M. Anderson *et al.*, EssE promotes Staphylococcus aureus ESS-dependent protein secretion to modify host immune responses during infection. *J. Bacteriol.* **199**, e00527-16 (2017).
39. V. Winstel, O. Schneewind, D. Missiakas, Staphylococcus aureus exploits the host apoptotic pathway to persist during infection. *mBio* **10**, e02270-19 (2019).
40. S. A. Plotkin, Vaccines: Correlates of vaccine-induced immunity. *Clin. Infect. Dis.* **47**, 401–409 (2008).
41. P. Bruhns, Properties of mouse and human IgG receptors and their contribution to disease models. *Blood* **119**, 5640–5649 (2012).
42. S. W. de Taeye, T. Rispens, G. Vidarsson, The ligands for human IgG and their effector functions. *Antibodies (Basel).* **8**, 30 (2019).
43. D. Ricklin, G. Hajishengallis, K. Yang, J. D. Lambris, Complement: A key system for immune surveillance and homeostasis. *Nat. Immunol.* **11**, 785–797 (2010).
44. E. T. Berends *et al.*, Distinct localization of the complement C5b–9 complex on Gram-positive bacteria. *Cell Microbiol.* **15**, 1955–1968 (2013).
45. C.-W. Vogel, D. C. Fritzinger, Cobra venom factor: Structure, function, and humanization for therapeutic complement depletion. *Toxicon.* **56**, 1198–1222 (2010).
46. M. Botto *et al.*, Homozygous C1q deficiency causes glomerulonephritis associated with multiple apoptotic bodies. *Nat. Genet.* **19**, 56–59 (1998).
47. F. Nimmerjahn, P. Bruhns, K. Horiuchi, J. V. Ravetch, FcgammaRIV: A novel FcR with distinct IgG subclass specificity. *Immunity* **23**, 41–51 (2005).
48. K. M. Cunnion, D. K. Benjamin Jr., C. G. Hester, M. M. Frank, Role of complement receptors 1 and 2 (CD35 and CD21), C3, C4, and C5 in survival by mice of Staphylococcus aureus bacteremia. *J. Lab. Clin. Med.* **143**, 358–365 (2004).
49. H. A. Verbrugh *et al.*, Staphylococcus aureus opsonization mediated via the classical and alternative complement pathways. A kinetic study using MgEGTA chelated serum and human sera deficient in IgG and complement factors C1s and C2. *Immunology* **36**, 391–397 (1979).
50. J. Lilue *et al.*, Sixteen diverse laboratory mouse reference genomes define strain-specific haplotypes and novel functional loci. *Nat. Genetics* **50**, 1574–1583 (2018).
51. D. C. Roopenian, S. Akilesh, FcRn: The neonatal Fc receptor comes of age. *Nat. Rev. Immunol.* **7**, 715 (2007).
52. K. M. Rigby, F. R. DeLeo, "Neutrophils in innate host defense against Staphylococcus aureus infections" in *Seminars in Immunopathology* (Springer, 2012), pp. 237–259.
53. T. R. Tipton *et al.*, Anti-mouse FcγRIV antibody 9E9 also blocks FcγRIII in vivo. *Blood.* **126**, 2643–2645 (2015).
54. S. Nigam *et al.*, Preclinical immunoPET imaging of glioblastoma-infiltrating myeloid cells using zirconium-89 labeled anti-CD11b antibody. *Mol. Imaging Biol.* **22**, 685–694 (2020).
55. R. Yuan, R. Clynes, J. Oh, J. V. Ravetch, M. D. Scharff, Antibody-mediated modulation of Cryptococcus neoformans infection is dependent on distinct Fc receptor functions and IgG subclasses. *J. Exp. Med.* **187**, 641–648 (1998).
56. N. Abboud *et al.*, A requirement for FcγR in antibody-mediated bacterial toxin neutralization. *J. Exp. Med.* **207**, 2395–2405 (2010).
57. M. R. Vogt *et al.*, Poorly neutralizing cross-reactive antibodies against the fusion loop of West Nile virus envelope protein protect in vivo via Fc-γ receptor and complement-dependent effector mechanisms. *J. Virol.* **85**, 11567–11580 (2011).
58. F. Nimmerjahn, J. V. Ravetch, Divergent immunoglobulin g subclass activity through selective Fc receptor binding. *Science* **310**, 1510–1512 (2005).
59. R. A. Robinett *et al.*, Dissecting FcgammaR regulation through a multivalent binding model. *Cell Syst.* **7**, 41–48.e5 (2018).
60. A. R. Cruz *et al.*, Toward understanding how *Staphylococca*l protein A inhibits IgG-mediated phagocytosis. *J Immunol* **209**, 1146–1155 (2022).
61. R. Sellers, C. Clifford, P. Treuting, C. Brayton, Immunological variation between inbred laboratory mouse strains: Points to consider in phenotyping genetically immunomodified mice. *Vet. Pathol.* **49**, 32–43 (2012).
62. C. Gillis, A. Gouel-Chéron, F. Jönsson, P. Bruhns, Contribution of human FcγRs to disease with evidence from human polymorphisms and transgenic animal studies. *Front. Immunol.* **5**, 254 (2014).
63. L. Ermini, I. Wilson, T. Goodship, N. Sheerin, Complement polymorphisms: Geographical distribution and relevance to disease. *Immunobiology* **217**, 265–271 (2012).
64. T. Kaifu, A. Nakamura, Polymorphisms of immunoglobulin receptors and the effects on clinical outcome in cancer immunotherapy and other immune diseases: a general review. *Int. Immunol.* **29**, 319–325 (2017).
65. N. Van Sorge, W. L. Van Der Pol, J. Van de Winkel, FcγR polymorphisms: Implications for function, disease susceptibility and immunotherapy. *Tissue Antigens* **61**, 189–202 (2003).
66. R. A. Floto *et al.*, Loss of function of a lupus-associated FcγRIIb polymorphism through exclusion from lipid rafts. *Nat. Med.* **11**, 1056–1058 (2005).
67. P. Bruhns *et al.*, Specificity and affinity of human Fcγ receptors and their polymorphic variants for human IgG subclasses. *Blood.* **113**, 3716–3725 (2009).
68. U. J. Sachs *et al.*, A variable number of tandem repeats polymorphism influences the transcriptional activity of the neonatal Fc receptor α-chain promoter. *Immunology* **119**, 83–89 (2006).
69. T. Billiet *et al.*, A genetic variation in the neonatal Fc-receptor affects anti-TNF drug concentrations in inflammatory bowel disease. *Am. J. Gastroenterol.* **111**, 1438–1445 (2016).
70. V. Gouilleux-Gruart *et al.*, Efficiency of immunoglobulin G replacement therapy in common variable immunodeficiency: correlations with clinical phenotype and polymorphism of the neonatal Fc receptor. *Clin. Exp. Immunol.* **171**, 186–194 (2013).
71. E. Racila *et al.*, A polymorphism in the complement component C1qA correlates with prolonged response following rituximab therapy of follicular lymphoma. *Clin. Cancer Res.* **14**, 6697–6703 (2008).
72. L. M. Rogers *et al.*, Complement-regulatory proteins CFHR1 and CFHR3 and patient response to anti-CD20 monoclonal antibody therapyCFHR1 and CFHR3 associate with anti-CD20 patient response. *Clin. Cancer Res.* **23**, 954–961 (2017).
73. C. Kerntke, F. Nimmerjahn, M. Biburger, There is (scientific) strength in numbers: A comprehensive quantitation of Fc gamma receptor numbers on human and murine peripheral blood leukocytes. *Front. Immunol.* **11**, 118 (2020).
74. T. S. Dodev *et al.*, A tool kit for rapid cloning and expression of recombinant antibodies. *Sci. Rep.* **4**, 5885 (2014).
75. P. A. Longo, J. M. Kavran, M.-S. Kim, D. J. Leahy, "Transient mammalian cell transfection with polyethylenimine (PEI)" in *Methods in Enzymology* (Elsevier, 2013), vol. 529, pp. 227–240.
76. L. Thomer *et al.*, Antibodies against a secreted product of *Staphylococcus aureus* trigger phagocytic killing. *J. Exp. Med.* **213**, 293–301 (2016).